Theoret. Chim. Acta (Berl.) 51, 65–78 (1979)

THEORETICA CHIMICA ACTA
© by Springer-Verlag 1979

Structure and Solvation of Nitrobenzene and 1,4-Dinitrobenzene Radical Anions

Jens Spanget-Larsen

Institut für Organische Chemie der Technischen Hochschule Darmstadt, Petersenstrasse 22, D-6100 Darmstadt, Federal Republic of Germany

An INDO method extended to include a contribution from the solvent by means of an effective solvent field (INDO-ESF) and based on properly optimized geometries is applied to the nitrobenzene and 1,4-dinitrobenzene radical anions. The hyperfine couplings and their solvent sensitivities are reproduced within a planar structure of the radicals. The behaviour of ^{14}N and ^{17}O splittings in derivatives with twisted nitro groups is accounted for with no difficulty.

Key words: INDO method with inclusion of an effective solvent field– Nitrobenzene and 1,4-dinitrobenzene radical anions, spin distribution and geometries of ~

1. Introduction

Few radicals have attracted the attention of ESR spectroscopists and theoreticians as nitrobenzene radical anions [1–20, 34]. A main reason for the continuing interest in these species is the unusually large sensitivity of the measured hyperfine couplings to structural and solvational perturbations. Adams *et al.* [2, 3] reported dramatic solvent dependence of the isotropic ^{14}N hyperfine constant a_N of the nitrobenzene radical anion $\mathbf{1}^{\dot{-}}$; a_N thus increased from 9.8 G in N,N-dimethylformamide (DMF) to 13.9 G in water (1 G = 10^{-4} Tesla). Similar increase of a_N was found by Geske and Ragle [4, 5] in ortho alkyl derivatives of $\mathbf{1}^{\dot{-}}$ where the nitro group is twisted out of the plane of the benzene ring. It was thus only natural very early to consider the possibility of a solvation induced twisting or other distortion of the nitro group as part of the explanation for the remarkable solvent sensitivity of a_N [3].

The first successful theoretical solvation model for organic π radicals was developed by Gendell, Freed and Fraenkel [6] on the basis of the Hückel theory and applied to nitroaromatic radicals by Rieger and Fraenkel [7]. They showed that the changes of

0040-5744/79/0051/0065/$02.80

a_N and a_H with the solvent in a series of nitroaromatic radicals could be well accounted for by Hückel calculations in which the oxygen Coulomb integral was increased with increasing solvent polarity. The effect of twisting the nitro group could similarly be reproduced by assuming a simple cosine relationship between the resonance integral for the C–N bond and the twist angle θ [5, 7]. Adams *et al.* [3] were able to conclude that even strong solvation as in water containing solvents does not show evidence of significant twisting of the nitro group, provided that the nitro group is essentially isolated spatially from other ring substituents. A solvation-induced twisting effect was found to be operative in radicals with substituents in positions ortho to the nitro group. No conclusions could be reached concerning other possible distortions of the nitro group, such as out-of-plane bending. Symons *et al.* [8, 9], however, suggested that the nitro group would undergo a pyramidal distortion as the spin density on nitrogen increased.

Later experimental investigations [10–15], in particular by Gulick and Geske and their coworkers, have made available several ^{17}O and ^{13}C coupling constants for the nitrobenzene and 1,4-dinitrobenzene radical anions $\mathbf{1}^{\dot{-}}$ and $\mathbf{2}^{\dot{-}}$ and their derivatives. The ^{17}O constants show a significant trend; in the case of $\mathbf{1}^{\dot{-}}$ and $\mathbf{2}^{\dot{-}}$ the magnitude increases slightly by increasing solvent polarity, but the trend is reversed in the pentamethyl derivative of $\mathbf{1}^{\dot{-}}$ where the nitro group is strongly hindered. Gulick and Geske [10, 11] interpreted the solvent dependence of a_O to mean that steric interactions are involved in the solvent effect, but were unable at the time to arrive at more definite conclusions.

The development of all-valence-electron molecular orbital (MO) procedures presented a new tool for the theoretical study of radicals [16, 17]. Gilbert and Trenwith [18] applied the INDO approximation [16] in an investigation of nitro radicals, but did not consider the influence of the solvent. This was attempted by Miller and Gulick [19] who studied hydrogen-bonded complexes between $\mathbf{1}^{\dot{-}}$ and water by means of INDO calculations. The results did not agree adequately with the experimental hyperfine data unless it was assumed that formation of a hydrogen-bond between water and the nitro group was accompanied by a pyramidal distortion of the nitro group. Investigation of the solvent dependence of a_{Cl}, however, indicated that the radical remained planar [13]. More promising results were obtained by a simple electrostatic solvation model within the INDO approximation, representing the interaction with the solvent by means of an effective solvent field (ESF) [20]; a preliminary application led to satisfactory agreement with the solvent sensitivities of the coupling constants of $\mathbf{1}^{\dot{-}}$ within the assumption of a planar structure of the radical.

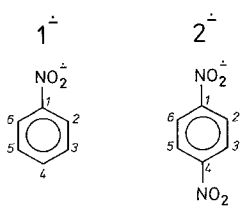

In this paper, the INDO-ESF approach is applied to $\mathbf{1}^{\dot{-}}$ and $\mathbf{2}^{\dot{-}}$, using geometries optimized by MINDO/3-UHF [21, 22], and, within a somewhat cruder scheme, to derivatives of $\mathbf{1}^{\dot{-}}$ and $\mathbf{2}^{\dot{-}}$ with twisted nitro groups. It will be shown that excellent agreement with all available hyperfine data is obtained within this framework.

2. The Effective Solvent Field (ESF) Model

An accurate description of the system defined by a solute molecule and the surrounding solvent medium is a difficult task, see, e.g., Refs. [23–26]. The problem is simplified enormously when energetic and dynamic aspects are neglected, and the interest is limited to the second-order polarization of the solute molecule due to interaction with the solvent. Further simplification is obtained by assuming that the interaction is purely electrostatic, as in the classical electrostatic solvation model [23, 24]. With regard to solvent polarization effects, this approach can be considered to be adequate; representation of specific interactions such as complex formation and steric effects in purely electrostatic terms is more problematic. It can be expected, however, that the effect of hydrogen-bonded complexes between solute and solvent can be represented within the electrostatic picture since the hydrogen-bond is of predominantly electrostatic nature [27].

In the effective solvent field (ESF) model [20, 28], the interaction with the solvent is described by assuming that solvent polarization and rapidly changing formation and breaking of complexes between solute and solvent give rise to an effective electric field, the ESF, at the position of the solute species. The effective electronic Hamiltonian of the molecule in solution is thus given by

$$H^{\mathrm{ESF}} = H + V^{\mathrm{ESF}}$$

where H is the Hamiltonian for the isolated molecule and V^{ESF} represents the potential due to the ESF. The ESF is conveniently approximated by a number of point charges q_{S}, in which case V^{ESF} takes the form

$$V^{\mathrm{ESF}} = -\sum_{i}^{\mathrm{electr.}} \sum_{\mathrm{S}} q_{\mathrm{S}}/r_{i\mathrm{S}}$$

This formulation is formally similar to an effective solute Hamiltonian within the theory of virtual charges (solvatons) [26]; but in the present context a simpler, essentially empirical approach is adopted. The empirical aspect is largely dictated by the need to incorporate the effect of specific interactions such as complex formation. In other words: the ESF model is an attempt to simulate "microscopic" "discrete" as well as "mascroscopic" "continuum" contributions [23, 25]. The ESF is modelled by an adequate arrangement of a minimum number of point charges q_{S} positioned outside the solute species and the magnitude of q_{S} is adjusted to obtain consistency with molecular observables and their solvent dependencies. This approach is suitable for molecules for which an "adequate" arrangement can be deduced from chemical knowledge. Favorable cases are molecules like semi-quinones and the nitroradicals with exposed, negatively charged oxygen centers, where the strong preference for solvation of these centers makes estimation of the

essential features of the ESF relatively straightforward [20, 28, 29]. But, of course, the ESF model is not capable of absolute predictions; the success of the model should be judged from its ability to predict trends and to correlate observed quantities and their solvent sensitivities. However, this limitation applies to any calculation of solvent effects based on a semiempirical procedure, and moreover, increasing the sophistication of the solvation model within the framework of approximate MO theory does not automatically increase the reliability of the results.

INDO calculations on $\mathbf{1}^{\dot{-}}$ and $\mathbf{2}^{\dot{-}}$ with inclusion of an ESF were carried out as described in detail previously [20]. One external point charge q was associated with each nitro group, positioned on the symmetry axis of the radical with $q\cdots O$ distances equal to 1.5 Å (1 Å $=10^{-10}$ m). The point charge was represented in the computer program [16, 30] by means of a pseudo proton with variable core charge q [20, 28], transmitting the ESF through the two-center electron repulsion integrals γ_{AB} ("neglect-of-penetration" in the INDO approximation [16]). Due to use of optimized geometries (Sect. 3) and introduction of the ESF, it is no longer adequate to apply the numerical factors relating isotropic hyperfine constants a_X to calculated valence s-type spin populations ρ_{Xns} in the original INDO parametrization [16]. The results are discussed directly in terms of the calculated ρ_{Xns} and their derivatives $\rho'_{Xns} = \partial\rho_{Xns}/\partial\Sigma q$, where Σq is the sum of the point charges q (i.e. q in the case of $\mathbf{1}^{\dot{-}}$, $2q$ in the case of $\mathbf{2}^{\dot{-}}$). The appropriate q values for $\mathbf{1}^{\dot{-}}$ and $\mathbf{2}^{\dot{-}}$ are not necessarily identical, but it is found that the same value is reasonably adequate in both cases. Comparison with observed coupling constants a_X and their solvent sensitivities a'_X indicates that the appropriate value of q is about $+\frac{1}{2}$e (1e = elementary charge $\approx 1.6022 \times 10^{-19}$ C).

3. Optimization of Geometry

In the present investigation of $\mathbf{1}^{\dot{-}}$ and $\mathbf{2}^{\dot{-}}$, their geometries have been calculated by the MINDO/3-UHF method [22]. Experimental investigations [31–33] indicate that neutral **1** is planar, but that the tendency towards planarity is the result of a delicate balance between oppositely directed contributions, resulting in a low internal rotation barrier for the nitro group [32, 33]. MINDO/3 is known to underestimate barriers towards rotation around single bonds [21, 29] and it is perhaps not surprising that the method in the case of **1** predicts a non-planar C_{2v} geometry, the planar structure being disfavored by 16.0 kJ/mole. Nevertheless, the MINDO/3-UHF calculation on the anion $\mathbf{1}^{\dot{-}}$ predicts a stable planar structure, in accordance with the result of a recent investigation of $\mathbf{1}^{\dot{-}}$ in single crystals of benzoate salts [34]. This result is explained by noting that the additional electron enters a strongly C–N bonding π-orbital, see Fig. 1, thereby increasing the formal C–N π-bond-order from 0.27 in (planar) **1** to 0.58 in $\mathbf{1}^{\dot{-}}$. This is reflected in a marked reduction of the C–N bond distance (Table 1) and a considerably increased tendency towards planarity. The geometry predicted for $\mathbf{2}^{\dot{-}}$ is slightly non-planar with a twist angle of 10°, but the planar structure is only 0.04 kJ/mole higher in energy. In view of what has been said above, this result can be interpreted to predict that $\mathbf{2}^{\dot{-}}$ is planar, but that the tendency towards planarity is less than in the case of

$\mathbf{1}^{\cdot-}$. This trend is in agreement with the relative C–N bonding characters of the orbitals in Fig. 1, but is in contradiction with the suggestion of Symons [8].

Table 1. Geometries of nitrobenzene **1** and 1,4-dinitrobenzene **2** and of their radical anions $\mathbf{1}^{\cdot-}$ and $\mathbf{2}^{\cdot-}$ calculated by MINDO/3 and MINDO/3-UHF, respectively (distances in Å)

	1	$\mathbf{1}^{\cdot-}$	**2**	$\mathbf{2}^{\cdot-}$
C1–N	1.434	1.362	1.443	1.382
N–O	1.229	1.263	1.226	1.247
C1–C2	1.431	1.464	1.426	1.456
C2–C3	1.404	1.395	1.404	1.378
C3–C4	1.405	1.417		
C2–H2	1.106	1.108	1.106	1.108
C3–H3	1.105	1.110		
C4–H4	1.105	1.107		
<O–N–O	129.4°	125.9°	130.2°	126.2°
<C6–C1–C2	116.6°	113.7°	116.0°	113.7°
<C1–C2–C3	121.5°	122.7°	122.0°	123.2°
<C2–C3–C4	120.5°	121.4°		
<C3–C4–C5	119.4°	118.1°		
<C1–C2–H2	122.2°	121.8°	115.7°	120.9°
<C4–C3–H2	120.1°	119.0°		
ΔH_f (kJ/mole)	51.3	−75.9	0.5	−229.2

The geometries calculated for **1**, $\mathbf{1}^{\cdot-}$, **2**, and $\mathbf{2}^{\cdot-}$ within the assumption of planar C_{2v} or D_{2h} symmetries are given in Table 1. An overall shift towards a quinoidal structure is predicted on addition of an electron, which is consistent with the shape and nodal properties of the acceptor orbitals as indicated in Fig. 1. The results in Table 1 refer to the gas phase and do not consider the strong solvation of $\mathbf{1}^{\cdot-}$ and $\mathbf{2}^{\cdot-}$ in solution. With respect to the spin distribution in these radicals, it can probably be assumed that the effect of the solvation on the molecular geometry is much less

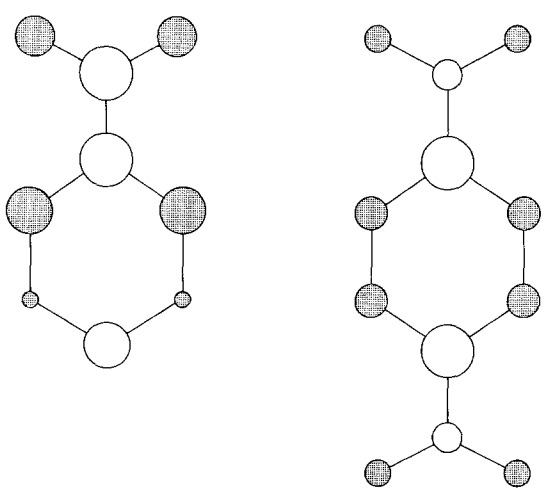

Fig. 1. Schematic representation of π MO amplitudes for the unpaired electron in $\mathbf{1}^{\cdot-}$ and $\mathbf{2}^{\cdot-}$ (MINDO/3-UHF)

important than the direct polarization of the electron density. The geometries given in Table 1 are thus considered as sufficiently adequate in this investigation.

4. Results and Discussion

4.1. *The Radical Anions* $\mathbf{1}^{\dot{-}}$ *and* $\mathbf{2}^{\dot{-}}$

Calculated valence *s*-type spin populations ρ_i obtained by the standard MINDO/3 and INDO UHF-Methods on the basis of the geometries discussed in the previous section are given in Table 2 (column 1–3), together with observed hyperfine data. It is not possible to correlate directly results for different nuclei, but consideration of results for, e.g., carbon positions shows that the calculations do not predict the relative magnitudes of the measured hyperfine coupling constants. Approximate annihilation of contaminating spin components of the single determinant MINDO/3 wave function does not improve the agreement since relative magnitudes are not affected. However, inclusion of the ESF in the INDO calculation as described in Sect. 2 influences drastically the calculated relative spin populations as shown in Fig. 2. Calculated results for $q = 0.5$e are included in Table 2 and are found

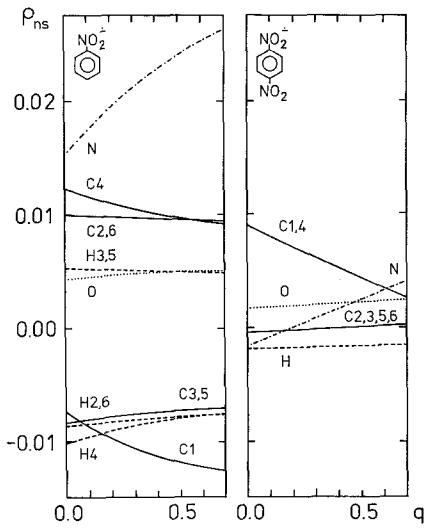

Fig. 2. Calculated valence *s*-type spin populations for $\mathbf{1}^{\dot{-}}$ and $\mathbf{2}^{\dot{-}}$ as a function of the ESF

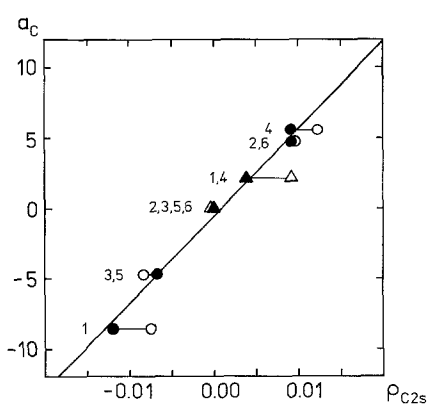

Fig. 3. Regression of observed ^{13}C coupling constants (G) on calculated C2*s* spin populations. Open points indicate results for $q = 0$, solid points results for $q = 0.5$e (Table 2). Circles and triangles indicate results for $\mathbf{1}^{\dot{-}}$ and $\mathbf{2}^{\dot{-}}$, respectively. The regression equation (solid points) is $a_C = -0.614 + 618.7\,\rho_{C2s}$; $R = 0.996$, S.E.E. = 0.43 G

Table 2. Calculated valence *s*-type spin populations ρ_i and their derivatives ρ_i' (see text), and observed ^{14}N, ^{17}O, ^{13}C, and ^{1}H hyperfine constants a_i and their solvent sensitivities $a_i' = \partial a_i / \partial X_{H_2O}$, where X_{H_2O} is the molar fraction of H_2O in a H_2O-DMF solvent mixture

Radical	i	MINDO/3[a]		INDO[b]	INDO-ESF[c]			Observed[d]		
		$\rho_i^{SD} \times 10^4$	$\rho_i^{AA} \times 10^5$	$\rho_i \times 10^4$	$\rho_i \times 10^4$	$\rho_i' \times 10^4$	ρ_i'/ρ_i	a_i	a_i'	a_i'/a_i
1$^{\cdot-}$	N	+246	+648	+150	+240	+125	+0.52	+11.3	+4.02	+0.36
	O	+18	+46	+43	+49	+6	+0.11	−8.9[e]	~ −0.6	~ +0.06
	C1	−183	−482	−75	−119	−49	+0.41	−8.5	−2.27	+0.27
	C2, 6	+338	+892	+99	+94	−8	−0.09	(+)4.7[f]	<0	<0
	C3, 5	−321	−849	−83	−73	+14	−0.19	(−)4.7[f]	>0	<0
	C4	+413	+1093	+122	+96	−33	−0.34	+5.6	−0.63	−0.11
	H2, 6	−330	−872	−87	−78	+12	−0.15	−3.3	~0	~0
	H3, 5	+238	+627	+52	+48	−6	−0.12	+1.1	~0	~0
	H4	−365	−965	−102	−80	+27	−0.34	−3.8	+0.53	−0.14
	$\langle S^2 \rangle$[g]	(1.036)	(0.815)							
2$^{\cdot-}$	N	+3	+10	−15	+25	+41	+1.63	+1.8	+1.45	+0.81
	O	+9	+29	+18	+23	+5	+0.21	−4.4[e]	~ −1.0	~ +0.2
	C1, 4	+187	+607	+91	+44	−45	−1.02	+2.0	~ −1.92	~ −0.96
	C2, 3, 5, 6	−1	−3	−3	+2	+4	+2.25	<|0.6|[h]	—	—
	H	−51	−166	−17	−15	+3	−0.19	−1.1	+0.01	−0.01
	$\langle S^2 \rangle$[g]	(0.790)	(0.750)							

[a] ρ_i^{SD} = single determinant value, ρ_i^{AA} = value obtained after app. annihilation of contaminating spin components [22].

[b] $q = 0$.

[c] $q = 0.5$e.

[d] Unless otherwise indicated, results from Refs. [12, 13] corresponding to $X_{H_2O} = 0.2$.

[e] Refs. [10, 11]; note that the moment of the ^{17}O nucleus is negative, producing *negative* coupling constants for *positive* spin density. X_{H_2O} = 0.1–0.2.

[f] Refs. [13, 14], $X_{H_2O} \sim 0$.

[g] Expectation value of the square of the total spin operator [22].

[h] Ref. [12], $X_{H_2O} = 0$.

to be in satisfactory agreement with the relative magnitudes of observed coupling constants for similar nuclei. In particular, the linear regression of the observed ^{13}C constants on the calculated ρ_{C2s} values is shown in Fig. 3. It is apparent that inclusion of the ESF leads to almost perfect correlation; the S.E.E. decreases from 1.62 G for $q=0$ to 0.43 G for $q=0.5$e. Results for $\mathbf{1}^{\dot{-}}$ and $\mathbf{2}^{\dot{-}}$ are well described by a single correlation line, indicating that $q=0.5$e is equally adequate in both cases.

It is clear that spin populations ρ_i at different positions are differently affected by the ESF in a way which leads to improved agreement with experiment. If this trend is significant, the sensitivity of ρ_i to variation of the ESF as represented by the derivative $\rho_i'=\partial\rho_i/\partial\Sigma q$ should reflect the behaviour of the corresponding coupling constant a_i on an increase of polarity of the medium. Experimental solvent sensitivities $a_i'=\partial a_i/\partial X_{H_2O}$, where X_{H_2O} is the molar fraction of water in a water-DMF solvent mixture, are included in Table 2. Again, direct comparison of results

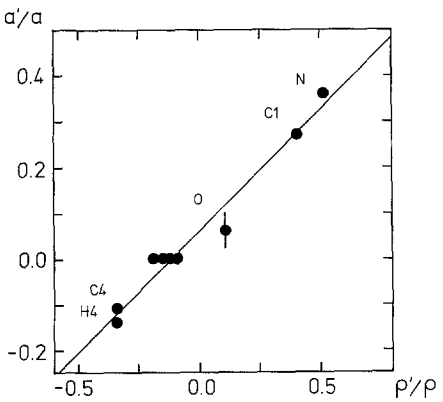

Fig. 4. Regression of observed quantities a'/a on calculated ρ'/ρ values for $\mathbf{1}^{\dot{-}}$ (Table 2). The regression line is $a'/a=0.060+0.525\,\rho'/\rho$; $R=0.984$, S.E.E. $=0.027\,X_{H_2O}^{-1}$

relating to different nuclei is not valid, but relative derivatives ρ_i'/ρ_i and a_i'/a_i should correlate without respect to type of nuclei. These quantities are given in Table 2 and the linear regression of a_i'/a_i on ρ_i'/ρ_i for all positions in $\mathbf{1}^{\dot{-}}$ is shown in Fig. 4. The quality of the correlation should be considered as highly satisfactory, particularly when it is recognized that the largest deviations occur for positions O and C3,5 where the experimental data are incomplete. The scatter of the experimental points for O [10] does not allow an accurate determination of a_O' (see Fig. 6), and detailed solvent studies of $a_{C3,5}$ and $a_{C2,6}$ are not available. The limited data published for the latter two [13, 14] indicate that the predicted signs of their solvent sensitivities are probably correct (Table 2).

The overall agreement demonstrated in Fig. 4 indicates that it is not necessary to invoke solvation induced twisting or other structural perturbations in order to account for the solvent sensitivity data for the hyperfine couplings of $\mathbf{1}^{\dot{-}}$. It is not particularly useful to include results for $\mathbf{2}^{\dot{-}}$ in the correlation in Fig. 4 because the prediction of very small spin populations ρ_i in some cases makes the ρ_i'/ρ_i values ill-defined. The spin populations at the C2, 3, 5, 6 and N positions thus change sign by an increase of q (Fig. 2, Table 1), rendering the ratio ρ_i'/ρ_i over-sensitive to variation

of q. However, comparison of calculated solvent sensitivities ρ_i' for $\mathbf{1}^{\dot{-}}$ and $\mathbf{2}^{\dot{-}}$ indicates that important trends are well predicted. The solvent sensitivity a_N' observed for $\mathbf{2}^{\dot{-}}$ is one third of the value observed for $\mathbf{1}^{\dot{-}}$, a ratio which is excellently reproduced by the calculated ρ_{N2s}' values, and also the magnitude of $a_{C1,4}'$ for $\mathbf{2}^{\dot{-}}$ relative to a_{C1}' and a_{C4}' for $\mathbf{1}^{\dot{-}}$ is well predicted by the model (Table 2).

It is possible that part of this excellent agreement is fortuitous, considering the overall empirical nature of this approach and the fact that $\mathbf{1}^{\dot{-}}$ and $\mathbf{2}^{\dot{-}}$ are differently shaped species which might differ with respect to solvation in a way not accounted for in the simple model. On the other hand, the consistency of the results for $\mathbf{1}^{\dot{-}}$ and $\mathbf{2}^{\dot{-}}$ indicates that the hyperfine data for these species can be explained without invoking the assumption of structural distortions.

4.2. Derivatives of $\mathbf{1}^{\dot{-}}$ *and* $\mathbf{2}^{\dot{-}}$ *with Twisted Nitro Groups*

In the remaining part of the paper, the effect of twisting the nitro group as in several alkyl derivatives of $\mathbf{1}^{\dot{-}}$ and $\mathbf{2}^{\dot{-}}$ is investigated. A somewhat cruder approach than in the previous paragraph is adopted. It is thus assumed that the influence of the alkyl groups on the spin distribution is due solely to a sterically induced twisting of the nitro groups. This assumption is justified by the observation that the hyperfine splittings in alkyl derivatives where the nitro group can remain in the in-plane position (e.g., *p*-derivatives) are relatively unaffected [4, 5]. Geometries are furthermore taken according to the regular scheme adopted by Pople *et al.* [16] and the expected lengthening of the C–N bond distance with increasing twist angle and increasing steric interference is not considered. With regard to solvation, it is assumed that methyl substitution does not influence drastically the shape of the ESF.

In Fig. 5 (left) is shown the influence of the twist angle θ on the calculated ρ_{N2s} value of $\mathbf{1}^{\dot{-}}$. Also the result for the 2-nitropropane radical anion is indicated; the result is an average of the ρ_{N2s} values obtained for the two conformations of C_s symmetry. The figure shows that ρ_{N2s} for $\mathbf{1}^{\dot{-}}$ is strongly increased with increasing θ, but that the solvent sensitivity as indicated by the dependence on q is correspondingly reduced. The solvent sensitivity predicted for θ values close to 90° is similar to the one predicted for the 2-nitropropane radical. This result is in disagreement with the prediction of Rieger and Fraenkel [7] that the solvent sensitivity should be essentially unaffected by the twist angle. In Fig. 5 (right) are shown observed results for $\mathbf{1}^{\dot{-}}$, 2,4,6-trimethyl-$\mathbf{1}^{\dot{-}}$, pentamethyl-$\mathbf{1}^{\dot{-}}$, and 2-nitropropane radical anion. The a_N values for the alkyl derivatives of $\mathbf{1}^{\dot{-}}$ increase with increasing steric hindrance of the nitro group, but the corresponding variation of the solvent sensitivity is not monotonic. The solvent sensitivity for the trimethyl derivative is by far the largest, in disagreement with the theoretical result for the assumption of a constant intermediate twist angle. This is most naturally explained by the conclusion of Adams *et al.* [3] that a pronounced solvation-induced twisting effect is operating in this radical; formation of hydrogen-bonded complexes with the solvent forces the sterically hindered nitro group to adopt even larger twist angles, resulting in the "extra" sensitivity of a_N when hydroxylic solvents are added. A similar effect may be

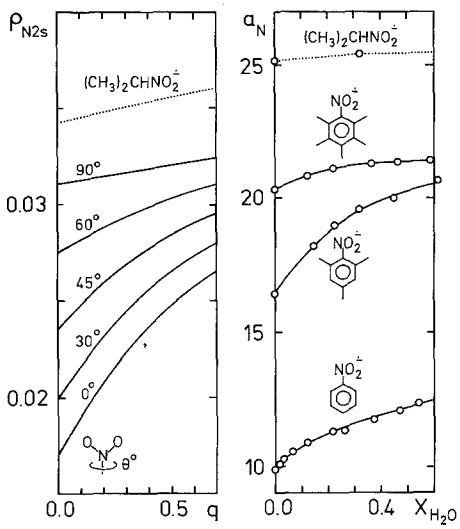

Fig. 5. (Left) Calculated N2*s* spin populations for $\mathbf{1}^{\dot{-}}$ for different twist angles θ as a function of the ESF. (Right) Observed ^{14}N coupling constants for $\mathbf{1}^{\dot{-}}$ and methyl derivatives of $\mathbf{1}^{\dot{-}}$ as a function of X_{H_2O} for a H_2O-DMF solvent mixture [3, 11, 13]. Results for 2-nitro-propane radical anion are indicated by dotted curves [3]

operative in the case of the pentamethyl derivative, but the twist angle in this highly hindered radical is probably so large that little is gained by further twisting. This is consistent with the fact that the solvent sensitivity for this radical is less than in the case of $\mathbf{1}^{\dot{-}}$, in agreement with the theoretical prediction without the need for the assumption of solvation-induced twisting.

The dependence of ρ_{N2s} on the twist angle θ as shown in Fig. 5 is such that for constant q, ρ_{N2s} is to a good approximation linearly related to $\cos^2\theta$. It is thus tempting to try a relation of the type

$$a_N(\theta) = a + b\cos^2\theta \tag{1}$$

in order to deduce effective twist angles from observed a_N values. The relation can be calibrated by estimating the limits of a_N for $\theta = 0°$ and $\theta = 90°$. It is simple to obtain a_N for zero twist angle, since this value can be taken from the result for $\mathbf{1}^{\dot{-}}$. The limit for $\theta = 90°$ is more difficult to obtain; inspection of Fig. 5 indicates that it may be reasonably safe to assume a value between 22 and 25 G. An approximate estimate of the effective twist angle θ is thus derived from (1) by the expression

$$\cos^2\theta = \frac{a_N(\theta) - 23.5 \pm 1.5}{a_N(0°) - 23.5 \pm 1.5} \tag{2}$$

For results in a pure DMF solvent the following θ values are obtained for the methyl derivatives in Fig. 5 (a_N in G):

	a_N	θ
$\mathbf{1}^{\dot{-}}$	9.7	(0°)
2,4,6-trimethyl-$\mathbf{1}^{\dot{-}}$	16.4	45 ± 3°
pentamethyl-$\mathbf{1}^{\dot{-}}$	20.3	62 ± 6°

and for a water-DMF mixture with $X_{H_2O}=0.5$:

	a_N	θ
$\mathbf{1}^{\dot{-}}$	12.1	(0°)
2,4,6-trimethyl-$\mathbf{1}^{\dot{-}}$	20.3	59±6°
pentamethyl-$\mathbf{1}^{\dot{-}}$	21.4	67±9°

These results indicate that a solvation induced twisting of 10–20° is consistent with the data for the trimethyl derivative. There appear to be at least two reasons for the exceptionally large solvent sensitivity of a_N for this radical (Fig. 5). In the first place, the twist angle induced by the methyl groups is considerable, but not so large that there is no room for a considerable solvent-induced twisting. Secondly, the effective twist angle in an aprotic solvent like DMF is probably in the range where the sensitivity of a_N to further twisting is maximal; according to (1), $\partial a_N/\partial\theta$ has a maximum for $\theta=45°$.

Twist angles for several methyl derivatives of $\mathbf{1}^{\dot{-}}$ estimated by means of Eq. (2) are given in Table 3, together with values estimated for the corresponding neutral

Table 3. Effective twist angles θ for the nitro group in methyl derivatives of $\mathbf{1}^{\dot{-}}$ and **1** estimated by means of Eq. (2) and the Braude-Sondheimer relationship [35], respectively

	$\mathbf{1}^{\dot{-}}$		**1**
Methyl derivative	a_N[a]	θ	θ[b]
Unsubstituted	10.3	(0°)	(0°)
2-	11.0	13±1°	34°
2,3-	11.7	19±1°	47°
2,6-	17.8	49±4°	66°
2,3,5,6-	20.4	62±6°	71°
2,3,4,5,6-	21.1	67±8°	—

[a] ^{14}N coupling constant in G measured in acetonitrile with ~1 mM water content [4, 5, 11].

[b] Taken from Wepster [36]; the data were derived from the 250 mμ absorption band in isoöctane..

compounds by means of the Braude-Sondheimer relationship $\cos^2\theta=\varepsilon/\varepsilon_0$ [35, 36], where ε is the molar absorbancy of the sterically hindered compound and ε_0 that of the planar reference analogue. The absolute magnitudes of the effective θ values in Table 3 should probably not be taken to seriously, but the trend towards lower twist angles for the radical anions relative to the corresponding neutral compounds, particularly for weakly hindered species, is probably a significant reflection of the increased tendency towards planarity expected on addition of an electron (Sect. 3).

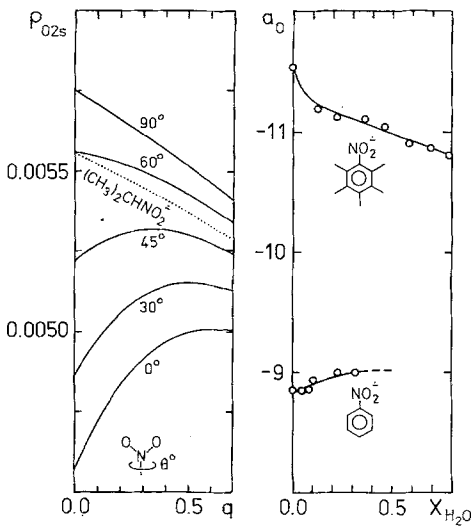

Fig. 6. This figure is the equivalent of Fig. 5 for ^{17}O [10, 11]

Fig. 6 is the equivalent of Fig. 5 for the oxygen positions. It is seen that the increase of $|a_O|$ and the change of sign of the solvent sensitivity observed when passing from $\mathbf{1}^{\cdot-}$ to pentamethyl-$\mathbf{1}^{\cdot-}$ are well reproduced in the model by an increase of twist angle, a result which is a significant success of the present approach. The results indicate that the variation of the sign of the solvent sensitivity can be explained in the following way. When the nitro group is strongly twisted out of the plane of the benzene ring, the influence of the solvent is largely a transfer of spin density from oxygen to nitrogen within the nitro group, rendering the solvent sensitivity of ρ_{O2s} negative. This is similar to the case of the 2-nitropropane radical anion (Fig. 6). Allowing the nitro group to conjugate with the phenyl group by reducing the twist angle, the limited transfer within the nitro group is gradually overruled by displacement of spin density from the benzene π system to the nitro group, resulting finally in a positive solvent sensitivity of ρ_{O2s}. This description is slightly oversimplified in so far as the π spin density on the oxygen atoms in planar $\mathbf{1}^{\cdot-}$ is predicted to *decrease* as the ESF is increased while the *s*-type spin density is simultaneously *increased* [20]. Within the framework of an empirical relation [10]

$$a_O = Q_1\rho_O^\pi + Q_2\rho_N^\pi$$

this can be interpreted to mean that the decrease of ρ_O^π as the radical environment is made more polar is overruled by the large increase of ρ_N^π.

Finally, a few results concerning a_N values in hindered alkyl derivatives of $\mathbf{2}^{\cdot-}$ are briefly discussed. Consider first the case where both nitro groups are twisted a similar amount. A considerable increase of a_N is observed, from 1.74 G in $\mathbf{2}^{\cdot-}$ to

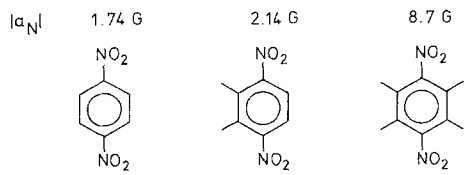

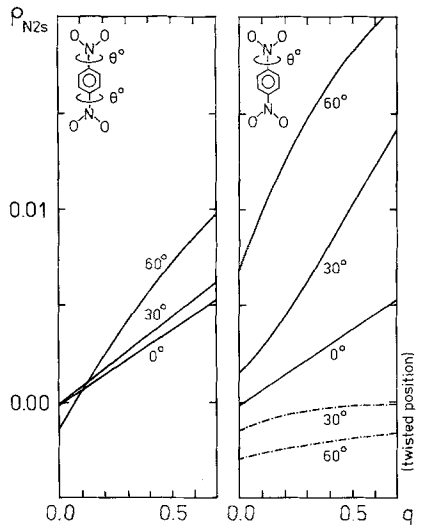

Fig. 7. Calculated N2*s* spin populations for $2^{\cdot-}$ for different twist angles θ as a function of the ESF. (Left) Twisting of both nitro groups. (Right) Twisting of one nitro group only

8.7 G in the highly hindered tetramethyl derivative [5]. The results of the INDO-ESF calculation is shown in Fig. 7 (left). It is interesting to note that the observed trend is not reproduced by the standard calculation ($q=0$), but agreement is obtained by inclusion of the ESF. The solvent sensitivity is predicted to increase with increasing twist angle, in contrast to the case of $\mathbf{1}^{\cdot-}$ (Fig. 5). In the case where only one nitro group is twisted out of the plane, a_N tends to be large for the

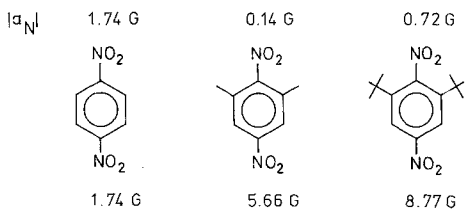

unhindered position and small for the twisted position [5]. Both magnitudes increase with increasing size of the alkyl group, an observation which puzzled Geske *et al.* [5] since one would expect the coupling constant for the hindered nitro group to decrease even further as the twist angle is increased. The observation finds a perfectly natural explanation by the assumption that a_N for the hindered position becomes *negative*, as indicated by the INDO-ESF results in Fig. 7 (right), at least in the case of 2,6-di-*t*-butyl-$\mathbf{2}^{\cdot-}$. Caution is in place, however, since the screening effect of the bulky *t*-butyl group can be expected to reduce the symmetry of the ESF and the results in Fig. 7 may not be reliable for this radical.

References

1. Geske, D. H.: Progr. Phys. Org. Chem. **4**, 125 (1967), and Refs. therein
2. Piette, L. H., Ludwig, P., Adams, R. N.: J. Am. Chem. Soc. **84**, 4212 (1962)
3. Ludwig, P., Layloff, T., Adams, R. N.: J. Am. Chem. Soc. **86**, 4568 (1964)

4. Geske, D. H., Ragle, J. L.: J. Am. Chem. Soc. **83**, 3532 (1961)
5. Geske, D. H., Ragle, J. L., Bambanek, M. A., Balch, A. L.: J. Am. Chem. Soc. **86**, 987 (1964)
6. Gendell, J., Freed, J. H., Fraenkel, G. K.: J. Chem. Phys. **37**, 2832 (1962)
7. Rieger, P. H., Fraenkel, G. K.: J. Chem. Phys. **39**, 609 (1963)
8. Symons, M. C. R.: Advan. Phys. Org. Chem. **1**, 283 (1963)
9. Fox, W. M., Gross, J. M., Symons, M. C. R.: J. Chem. Soc. (A) 448 (1966); Gross, J. M., Symons, M. C. R.: J. Chem. Soc. (A) 451 (1966)
10. Gulick, W. M., Jr., Geske, D. H.: J. Am. Chem. Soc. **87**, 4049 (1965)
11. Gulick, W. M., Jr., Geiger, W. E., Jr., Geske, D. H.: J. Am. Chem. Soc. **90**, 4218 (1968)
12. Parrish, R. G., Hall, G. S., Gulick, W. M., Jr.: Mol. Phys. **26**, 1121 (1973)
13. Swartz, G. L., Gulick, W. M., Jr.: Mol. Phys. **30**, 869 (1975)
14. Schreiner, K., Lotz, A., Aurich, H. G., Berndt, A.: Tetrahedron **31**, 2117 (1975)
15. Gulick, W. M., Jr., Swartz, G. L., Parrish, R. G.: J. Magn. Reson. **22**, 81 (1976)
16. Pople, J. A., Beveridge, D. L., Dobosh, P. A.: J. Am. Chem. Soc. **90**, 4201 (1968); Pople, J. A., Beveridge, D. L.: Approximate molecular orbital theory. New York: McGraw-Hill 1970
17. Beveridge, D. L., in: Semiempirical methods of electronic structure calculations, Part B, Chapt. 5, Segal, G. A., ed. New York: Plenum Press 1977
18. Gilbert, B. C., Trenwith, M.: J. Chem. Soc. Perkin II 2010 (1973)
19. Miller, C., Gulick, W. M., Jr.: Mol. Phys. **27**, 1185 (1974)
20. Spanget-Larsen, J.: Mol. Phys. **32**, 735 (1976)
21. Bingham, R. C., Dewar, M. J. S., Lo, D. H.: J. Am. Chem. Soc. **97**, 1302 (1975), and subsequent papers
22. Bischof, P.: J. Am. Chem. Soc. **98**, 6844 (1976)
23. McGreery, J. H., Christoffersen, R. E., Hall, G. G.: J. Am. Chem. Soc. **98**, 7191, 7196 (1976)
24. Birnstock, F., Hofmann, H.-J., Köhler, H.-J.: Theoret. Chim. Acta (Berl.) **42**, 322 (1976)
25. Claverie, P., Daudey, J. P., Langlet, J., Pullman, B., Piazzola, D., Huron, M. J.: J. Phys. Chem. **82**, 405 (1978)
26. Constanciel, R., Tapia, O.: Theoret. Chim. Acta (Berl.) **48**, 75 (1978)
27. Dolgushin, M. D., Pinchuk, V. M.: Theoret. Chim. Acta (Berl.) **45**, 157 (1977)
28. Spanget-Larsen, J.: Theoret. Chim. Acta (Berl.) **47**, 315 (1978)
29. Spanget-Larsen, J.: Chem. Phys. Letters **44**, 543 (1976)
30. Quantum Chemistry Program Exchange, Indiana University: QCPE 141
31. Trotter, J.: Acta Cryst. **12**, 884 (1959)
32. Høg, J., Nygaard, L., Sørensen, G. O.: J. Mol. Struct. **1**, 111 (1970)
33. Carreira, L. A., Towns, T. G.: J. Mol. Struct. **41**, 1 (1977)
34. Mason, R. P., Harriman, J. E.: J. Chem. Phys. **65**, 2274 (1976)
35. Braude, E. A., Sondheimer, F.: J. Chem. Soc. 3754 (1955)
36. Wepster, B. M., in: Progress in stereochemistry, Vol. 2, Chapt. 4, Klyne, W., de la Mare, P. B. D., eds. London: Butterworths 1958

Received July 10, 1978/September 13, 1978